



# Phreatic and Hydrothermal Eruptions: From Overlooked to Looking Over

Cristian Montanaro<sup>1,2</sup> · Emily Mick<sup>3</sup> · Jessica Salas-Navarro<sup>3</sup> · Corentin Caudron<sup>4</sup> · Shane J. Cronin<sup>2</sup> · J. Maarten de Moor<sup>5,6</sup> · Bettina Scheu<sup>1</sup> · John Stix<sup>3</sup> · Karen Strehlow<sup>7</sup>

Received: 15 July 2021 / Accepted: 6 May 2022 / Published online: 2 June 2022  
© The Author(s) 2022

## Abstract

Over the last decade, field investigations, laboratory experiments, geophysical exploration and petrological, geochemical and numerical modelling have provided insight into the mechanisms of phreatic and hydrothermal eruptions. These eruptions are driven by sudden flashing of ground- or hydrothermal water to steam and are strongly influenced by the interaction of host rock and hydrothermal system. Aquifers hosted in volcanic edifices, calderas and rift environments can be primed for instability by alteration processes affecting rock permeability and/or strength, while magmatic fluid injection(s), earthquakes or other subtle triggers can promote explosive failure. Gas emission, ground deformation and seismicity may provide short- to medium-term forerunner signals of these eruptions, yet a definition of universal precursors remains a key challenge. Looking forward in the next 10 years, improved warning and hazard assessment will require integration of field and experimental data with models combining case studies, as well as development of new monitoring methods integrated by machine learning approaches.

**Keywords** Phreatic eruptions · Hydrothermal eruptions · Triggers · Dynamics · Forecasting

---

This paper constitutes part of a topical collection:

Looking Backwards and Forwards in Volcanology: A Collection of Perspectives on the Trajectory of a Science

Editorial responsibility: K. V. Cashman

---

✉ Cristian Montanaro  
cristian.montanaro@min.uni-muenchen.de

<sup>1</sup> Department of Earth and Environmental Sciences, Ludwig-Maximilians-Universität München, Munich, Germany

<sup>2</sup> School of Environment, University of Auckland, Auckland, New Zealand

<sup>3</sup> Department of Earth & Planetary Sciences, McGill University, Montreal, Canada

<sup>4</sup> Laboratoire G-Time, Department of Geosciences, Environment and Society, Université Libre de Bruxelles, Bruxelles, Belgium

<sup>5</sup> Observatorio Vulcanológico Y Sismológico de Costa Rica, Universidad Nacional, Heredia, Costa Rica

<sup>6</sup> Department of Earth and Planetary Sciences, University of New Mexico, Albuquerque, NM, USA

<sup>7</sup> GEOMAR Helmholtz Centre for Ocean Research, Kiel, Germany

## Introduction

Phreatic and hydrothermal eruptions are explosive phenomena ubiquitous to volcanoes, calderas and tectonic rifts areas (Browne and Lawless 2001). Phreatic eruptions are produced by explosive expansion of groundwater due to the sudden arrival of heat and gas from intruding magma (or magmatic fluids), whereas hydrothermal eruptions result from the flashing and expansion of hydrothermal water without the need for any magmatic input (Mastin 1995; Browne and Lawless 2001; Thiéry and Mercury 2009). Despite their comparatively small size, these eruptions can be deadly as they often lack precursors (Barberi et al. 1992; Hurst et al. 2014; Stix and de Moor 2018). When occurring, precursors are too weak, initiate only shortly before the eruption onset or affect a small localised area that cannot be detected with normal monitoring networks (Jolly et al. 2014; Dempsey et al. 2020). As a result, useful forecasts cannot be made. Absent or ambiguous signals may be related to temporal and spatial scales of priming and precursory processes as in the case, for example, of slow accumulation of magmatic gas within aquifers (Sano et al. 2015; Battaglia et al. 2019), or rapid heating and pressurisation of a small volume of

fluids (Christenson et al. 2010; Kobayashi et al. 2018). This may result in gradual development of pressurised aquifers over long timescales versus fast and dynamic interaction of ascending magmatic fluids with the existing aquifer involving cold and/or hydrothermal water, where short-term precursory signals can be present (Chiodini et al. 1995).

Here we discuss advances in processes, characteristics, triggers and lithological factors influencing fragmentation and eruptive dynamics of phreatic and hydrothermal eruptions on observed or monitored eruptions from the past ten years. Different precursory signals and their meaning are explained in the light of their source mechanisms and geological context. A number of unanswered questions about triggering and forecasting these eruptions, as well as future directions and perspectives, are also presented. A video footage of an unheralded phreatic eruption at Rincón de la Vieja (Costa Rica), and a full library sorted and collated into 17 thematic topics covering the last ten years of research are supplied in the Online Resources.

## Key events of the past 10 years

Researchers have long struggled to provide consistent definitions and genetic criteria for phreatic and hydrothermal eruptions (Browne and Lawless 2001; Montanaro et al. 2016c; Stix and de Moor 2018). This problem is further exacerbated by the similarity of their dynamics and deposits with those from phreatomagmatic eruptions involving small amounts of magma, and occurring at “wet” volcanoes where vent-hosted hydrothermal systems are common (Pardo et al. 2014; Alvarado et al. 2016; Christenson et al. 2017). It also must be recognised that one eruption type can transition into another in just a few minutes (Swanson et al. 2014; Battaglia et al. 2019). These eruptions can last from seconds to hours, eject large ballistics, generate highly energetic steam-rich density currents (surges) and expel wet jets of poorly sorted rock debris (Lube et al. 2014; Maeno et al. 2016; Kilgour et al. 2019). Deposits are generally of low volume ( $< 10^6 \text{ m}^3$ ) and restricted to within hundreds of metres to a few kilometres from crater margins, while resulting craters range from a few metres up to hundreds of metres in diameter, with depths from few to several hundred metres (Kilgour et al. 2010; Breard et al. 2014; Montanaro et al. 2016b; Strehlow et al. 2017; Terada et al. 2021). As summarised in Table 1, more than 30 phreatic and hydrothermal eruptions were observed during 2011–2021. The example of a video obtained during the recent phreatic eruption at Rincón de la Vieja in Costa Rica (Online Resources 1) shows the unpredictable nature of these types of explosive events, and how fast products can be dispersed over wide areas. In addition, hundreds of studies published during the last decade have provided insight that elucidate their triggering mechanisms and eruptive

processes (Online Resources 2). Illustrative events during the past 10 years include:

- On September 27, 2014, the rupture of a hydrothermal seal produced a phreatic eruption at Mt. Ontake (Japan), killing 63 people (Kato et al. 2015; Kaneko et al. 2016). Long-period and volcano-tectonic earthquakes were detected September 6–11, resuming 10 min prior to eruption (Zhang and Wen 2015; Kaneko et al. 2016). A slight deviation in the stress field was observed a week before the eruptive event; ground inflation of the volcanic edifice occurred seven minutes before the eruption (Terakawa et al. 2016). The eruption launched ballistics reaching a distance of  $\sim 1 \text{ km}$ , produced a 7 km-high ash plume and generated low-temperature pyroclastic density currents (Kaneko et al. 2016; Oikawa et al. 2016).
- On April 27, 2016, Whakaari/White Island (New Zealand) produced a phreatic eruption generating a small pyroclastic density current following weak tremors and decreasing crater lake levels (Hamling 2017; Walsh et al. 2019; Kilgour et al. 2019; Caudron et al. 2021). On December 9, 2019, seismic activity and  $\text{SO}_2$  flux increased  $\sim 40 \text{ min}$  before another eruption that produced a 3–4 km-high ash plume and warm ( $< 100 \text{ }^\circ\text{C}$ ) pyroclastic density currents that killed 21 people and injured 26 (Dempsey et al. 2020; Burton et al. 2021).
- A hydrothermal eruption at Te Maari/Tongariro (New Zealand) occurred on August 6, 2012, following seismic unrest between July 13 and August 1, which resumed 5 min prior to the eruption (Hurst et al. 2014; Jolly et al. 2014). A landslide unroofed the over-pressured and sealed hydrothermal system producing a 7 km-high plume and warm ( $\sim 80 \text{ }^\circ\text{C}$ ) pyroclastic density currents (Lube et al. 2014; Pardo et al. 2014). A second smaller eruption occurred without precursors on November 21, 2012, and was observed and recorded by tourists (Erfurt-cooper 2014).

Ejected ash from the Te Maari’s August eruption included glassy fragments among the mechanically fragmented host rock (lavas and pyroclasts). The difficulty in identifying fresh juvenile pyroclasts in fine ash deposits raised the questions about the capability to discern juvenile products in small phreatomagmatic eruptions and requires rethinking of the long-standing definition of phreatic and hydrothermal as eruptions involving no magmatic material (Pardo et al. 2014).

Some volcanoes experience periods of prolonged activity with alternating or consecutive phreatic and phreatomagmatic events. For instance, between 2014 and 2020 Turrialba (Costa Rica) produced frequent eruptions of these types due to magma injection and/or breaking of

**Table 1** List of phreatic, hydrothermal, and phreatomagmatic eruptions from the last 10 years. Settings, processes, triggers, characteristics, products and timing are summarised

Site	Date	Eruption type/ geologic/litho- logic setting	Juvenile material present	Processes	Triggers	Characteristics	Volume/area/crater size(s)	Unrest to activity timing	References
Ontake (Japan)	September 27, 2014	Phreatic / Volcano flank (lava, pyroclastic deposits)	Yes; <0.7 wt% glassy particles	Rupture of a hydrothermal seal	Injection mag- matic gas	Ballistics shower (up to ~1 km); ash plume (7 km); low-T PDC	Ballistic field, ash plume, PDC <i>Volume (tot):</i> 0.7– 1.3 × 10 <sup>6</sup> m. <sup>3</sup> <i>Area:</i> 2, ~ 1200, 3 km. <sup>2</sup> <i>Crater size(s):</i> <50–150 m	<i>Mid-term:</i> Crus- tal deformation (1 month); LP and VT earthquakes (21 days) <i>Short-term:</i> VT earthquakes, seismic tremor, and ground inflation (< 10 min)	1–5
Te Maari/ Tongariro (New Zealand)	August 6, 2012	Hydrothermal / Volcano flank (breccias, brecciated- tuffs, lavas)	No	Unroofing of hydrothermal system	Landslide	Ballistics shower (up to ~ 1.4 km); ash plume (7.8–10 km); low-T PDC	Ballistic field, ash plume, PDC <i>Volume:</i> > 200, 2.3– 2.8 × 10 <sup>5</sup> , 3.4 × 10 <sup>5</sup> m. <sup>3</sup> <i>Area:</i> 5.1, > 6000, 6.1 km. <sup>2</sup> <i>Crater size:</i> > 400 × 65 × 15 m	<i>Long-term:</i> change in seis- mic attenuation (Months) <i>Mid-term:</i> Seis- mic swarms (20 days)	6–10
	November 21, 2012	Hydrothermal	No	Unknown	Unknown	Ballistics shower (< 0.2 km); ash plume (3–5 km); low T PDC	Unknown	No precursor	11
Whakaari/ White Island (New Zealand)	April 27, 2016	Phreatic / Vent-hosted (unconsolidated pyroclastic deposits)	No	Rupture of a hydrothermal seal	Injection mag- matic gas	Ballistics shower (up to ~ 0.3 km); low-T PDC	Ballistic field, PDC <i>Volume (tot):</i> 1.3 × 10 <sup>4</sup> m. <sup>3</sup> <i>Area:</i> 0.1, 0.33 km. <sup>2</sup> <i>Crater size:</i> < 50 m	<i>Long-term:</i> Ground defor- mation, change in seismic attenuation (months) <i>Mid-term:</i> Lake drainage (2 weeks) <i>Short-term:</i> VLP (2 h)	12–15
	December 19, 2019	Phreatic/ hydrothermal	Unknown	Rupture of a hydrothermal seal	Injection mag- matic gas	Ballistics shower; gas and ash plume (4 km); low-T PDC	Unknown	<i>Short-term:</i> Increased SO <sub>2</sub> flux, plume height, and seismic tremor (~ 40 min)	16, 17

Table 1 (continued)

Site	Date	Eruption type/ geologic/litho- logic setting	Juvenile material present	Processes	Triggers	Characteristics	Volume/area/crater size(s)	Unrest to activity timing	References
Kverkfjöll / Gengissig (Iceland)	August 15, 2013	Hydrothermal / Caldera (unconsolidated lake sediments)	No	Rupture of low-permeable clay-rich seal	Lake drainage	Ballistics shower; ash plume ( $< 0.1$ km);	Ballistic field, ash plume <i>Volume (tot)</i> : $8 \times 10^3$ m. <sup>3</sup> <i>Area (tot)</i> : $0.3$ km. <sup>2</sup> <i>Crater size</i> : 9–20 m	No precursor	18
Ebinokogen Ioyama (Japan)	April 19, 2018	Hydrothermal / Volcano flank (unconsolidated pyroclastic deposits)	No	Rupture of a hydrothermal seal	Injection hydro- thermal fluids	Ballistic launch ( $< 100$ m); gas and ash jet (100–200 m)	Ballistic field, ash plume <i>Volume</i> ( <i>tot</i> ): $1.5 \times 10^3$ m. <sup>3</sup> <i>Area (tot)</i> : $0.04$ km. <sup>2</sup> <i>Crater size</i> : 9–37 m	<i>Long-term</i> : Ground ther- mal anomalies, spring T°C increase (2 yrs); fumarole T°C increase (1 yr.); fluid kick at a fuma- role (1 yr.)	19,20
Turrialba (Costa Rica)	2011–2021 (9 eruptive phases)	Phreatic-phreato- magmatic / Vent-hosted (lava, pyroclastic deposits)	Yes: $< 10\%$ fresh glass	Rupture of a hydrothermal seal	Injection mag- matic gas	Repeated ash plumes (0.1–2.5 km), near constant gas emissions	Ballistic field, ash plume <i>Volume</i> : variable <i>Area</i> : variable <i>Crater size</i> : 200 m	<i>Long-term</i> : Seis- mic swarms, increased fumarolic activity (8 years) <i>Mid-term</i> : Increased CO <sub>2</sub> / SO <sub>2</sub> , decreased H <sub>2</sub> S/SO <sub>2</sub> (1–3 weeks) <i>Short-term</i> : Seismic tremor (hours-days)	21,22
Rincón de la Vieja (Costa Rica)	2011–2021 (9 eruptive phases)	Phreatic-phreato- magmatic / Vent-hosted Crater Lake (lava, pyroclastic deposits)	Yes: 1–44% fresh glass	Rupture of a hydrothermal seal	Injection mag- matic gas	Repeated ash plumes (0.1–2 km), repeated lahar ( $< 10$ km)	Ballistic field, ash plume, lahar <i>Volume</i> : variable <i>Area</i> : variable <i>Crater size</i> : 500 m	<i>Long-term</i> : Increased fumarolic and seismic activity (6 months)	23

Table 1 (continued)

Site	Date	Eruption type/ geologic/litho- logic setting	Juvenile material present	Processes	Triggers	Characteristics	Volume/area/crater size(s)	Unrest to activity timing	References
Hakone (Japan)	June 29, 2015	Phreatic / Volcano flank (pyroclastic deposits)	No	Deformation and extensional crack opening	Injection magmatic gas (CO <sub>2</sub> )	Ballistic launch (<30 m); gas and ash jet (unknown), mud- and debris flow (~150 m)	Ballistic field, ash plume <i>Volume (tot)</i> : $1 \times 10^2$ m. <sup>3</sup> <i>Area (tot)</i> : <0.02 km. <sup>2</sup> <i>Crater size</i> : ≤15 m	<i>Long-term</i> : Ground defor- mation, seismic swarm, thermal anomalies (3 months) <i>Mid-term</i> : Intense steam- ing ground, seismic swarms (1–2 weeks) <i>Short-term</i> : Seismic tremor (2 h)	24,26
Poás (Costa Rica)	2011–2017 (6 eruptive phases)	Phreatic Vent-hosted Crater Lake (pyroclastic deposits)	No	Rupture of a hydrothermal seal below a crater lake	Injection mag- matic gas (CO <sub>2</sub> and SO <sub>2</sub> )	Gas bursts to vertical jets of solids and flu- ids (10–400 m), radial base surge of vapour (<150 m)	Ballistics, ash plume <i>Volume</i> : variable <i>Area</i> : <0.06 km. <sup>2</sup> <i>Crater size</i> : unknown	<i>Short-term</i> : fluc- tuations in lake gas composi- tion (24–36 h)	27,28
Kusatsu-Shirane (Motoshirane) (Japan)	January 23, 2018	Phreatic / Volcano flank (pyroclastic deposits)	No	Breaking of seals or weak levels along a fault	Injection hydro- thermal fluids	Ballistic launch (0.5 km); ash plume (3.4 km)	Ballistic field, ash plume <i>Volume (tot)</i> : 3.4– 4.9 × 10 <sup>4</sup> m. <sup>3</sup> <i>Area</i> : 0.5, <100 km. <sup>2</sup> <i>Crater size</i> : 500 m long craters row	<i>Long-term</i> : Ground deformation, seismic swarm (4 years) <i>Short-term</i> : Volcanic tremor and tilt deformation (~2 min)	29,30

1. Kaneko et al. 2016; 2. Oikawa et al. 2016; 3. Miyagi et al. 2020; 4. Terakawa et al., 2016; 5. Zhang and Wen, 2015; 6. Hurst et al. 2014; 7. Jolly et al. 2014b; 8. Pardo et al. 2014; 9. Lube et al. 2014; 10. Caudron et al., 2019; 11. Erfurt-cooper 2014; 12. Jolly et al. 2018; 13. Kilgour et al. 2019; 14. Walsh et al. 2019; 15. Caudron et al., 2021; 16. Burton et al. 2021; 17. Dempsey et al. 2020; 18. Montanaro et al. 2016b; 19. Tajima et al. 2020; 20. Ohba et al. 2021; 21. Mick et al. 2021; 22. Rouwet et al. 2021; 23. Battaglia et al. 2019, 24. Doke et al. 2018; 25. Kobayashi et al. 2018; 26. Narita et al. 2020; 27. de Moor et al. 2016; 28. Salvage et al. 2018; 29. Matsunaga et al. 2020; 30. Yamada et al. 2021

hydrothermal sealing that generated ash plumes up to 4 km high (Alvarado et al. 2016; de Moor et al. 2016; Stix and de Moor 2018; DeVitre et al. 2019).

The complexity in the processes, sources and dynamics of these eruptions is striking. Therefore, we suggest that explosive events with a hydrological component occur on a spectrum between three end-members: phreatic, hydrothermal and phreatomagmatic. Combining a number of observations from different volcanic systems, we propose a conceptual classification for different eruption types (Fig. 1, Table 1). The presence of juvenile material is a key feature to identify phreatomagmatic events, whereas phreatic and hydrothermal origins can be defined by considering: i) energetic source type, ii) hydrologic setting, iii) erupted lithology, iv) triggers and v) timescale between any magmatic perturbation and hydrothermal system response.

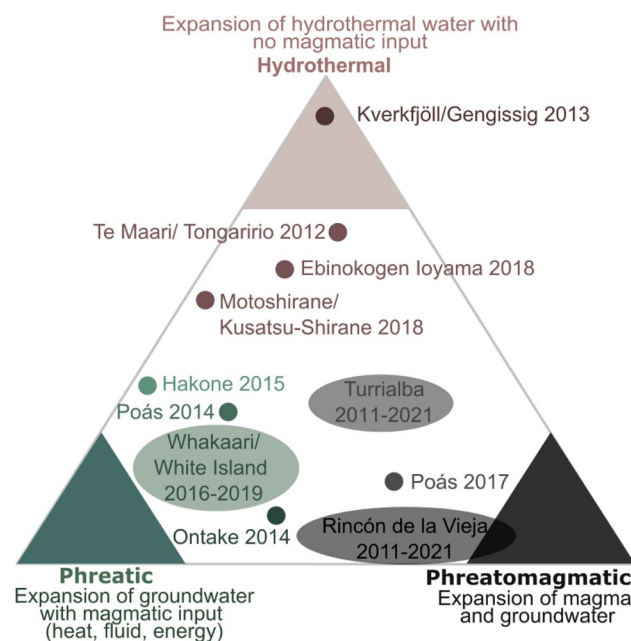


**Fig. 1** Ternary diagram illustrating the conceptual classification of volcanic eruptions resulting from the explosive expansion of water with phreatic, hydrothermal and phreatomagmatic end-members. Significant eruptions over the last 10 years are plotted qualitatively: Te Maari/Tongariro August 6, 2012, Ontake September 27, 2014, Poás February–October 2014, Ebinokogen Ioyama April 19, 2018, Hakone June 29, 2015, Kverkfjöll/Gengissig August 16, 2013, Whakaari/White Island 2016–2019, Poás April 14, 2017, Turrialba 2011–2021, Rincón de la Vieja 2011–2021 (see also Table 1). Differentiation between end-members is based on qualitative assessment of the: i) presence and proportion of juvenile material indicative for phreatomagmatic contributions, ii) identification of injected fluids—when present—and their abundance to discriminate magmatic input, iii) hydrologic setting indicative of the balance between hydrothermal and groundwater, iv) presence of an active hydrothermal aquifer and its relative size indicative of the proportion of hydrothermal contributions, v) erupted lithologies, vi) triggering mechanism and vii) timescale between any external perturbations and aquifer response

## Processes, triggers and characteristics

### Priming and eruption controlling parameters

Phreatic and hydrothermal eruptions are powered by the sudden conversion of thermal energy stored in fluids into mechanical work (rock fragmentation and particle ejection). The main factors controlling the preparatory state (priming) of both fluids and host reservoir, as well as the fragmentation and ejection mechanisms, include:

1. The pressure/temperature differential from source region to ambient surface conditions and the rate of pressure release (Thiéry and Mercury 2009; Montanaro et al. 2016a);
2. The state of the fluid (gas, liquid, gas + liquid) and its volume (Mastin 1995; Ohba et al. 2007; Thiéry and Mercury 2009; Toramaru and Maeda 2013; Montanaro et al. 2016c, a; Fullard and Lynch 2012);
3. The geometry and properties (connected porosity, permeability and strength) of the aquifer host rock (Haug et al. 2013; Galland et al. 2014; Mayer et al. 2016; Kennedy et al. 2020; Montanaro et al. 2021a, b; Fullard and Lynch 2012).

The first two factors define the overpressure conditions and the bulk mechanical energy available during an eruption, which could also be augmented by additional dissolved gases (e.g. CO<sub>2</sub>) that lower the liquid stability limit (Thiéry and Mercury 2009; Thiéry et al. 2010; Hurwitz et al. 2016). The third factor influences the style of an eruption, as well as its intensity via the relative partitioning of energy between work of rock fragmentation versus conversion into kinetic energy (Raue 2004; Montanaro et al. 2016b, 2021a; Rosi et al. 2018; Kilgour et al. 2019).

### Geological settings

Phreatic and hydrothermal eruptions can occur in volcanic and vent-hosted hydrothermal systems, as well as in active geothermal fields within calderas or volcano-tectonic rifts (Fig. 2, Table 1). Aquifers can be “primed” for eruption by sealing via hydrothermal alteration and mineralisation, including build-up of pore/fracture-filling sulphates, clays, sulphur minerals and silica (Gurioli et al. 2012; Sutawidjaja et al. 2013; Heap et al. 2019; Gaete et al. 2020; Mick et al. 2021). However, sealing can be localised or affect extensive areas in these diverse geological environments and occur progressively or suddenly, as well as can be contrasted by rapid permeability increase (e.g. fracturing). Therefore, changes in aquifer conditions can occur over

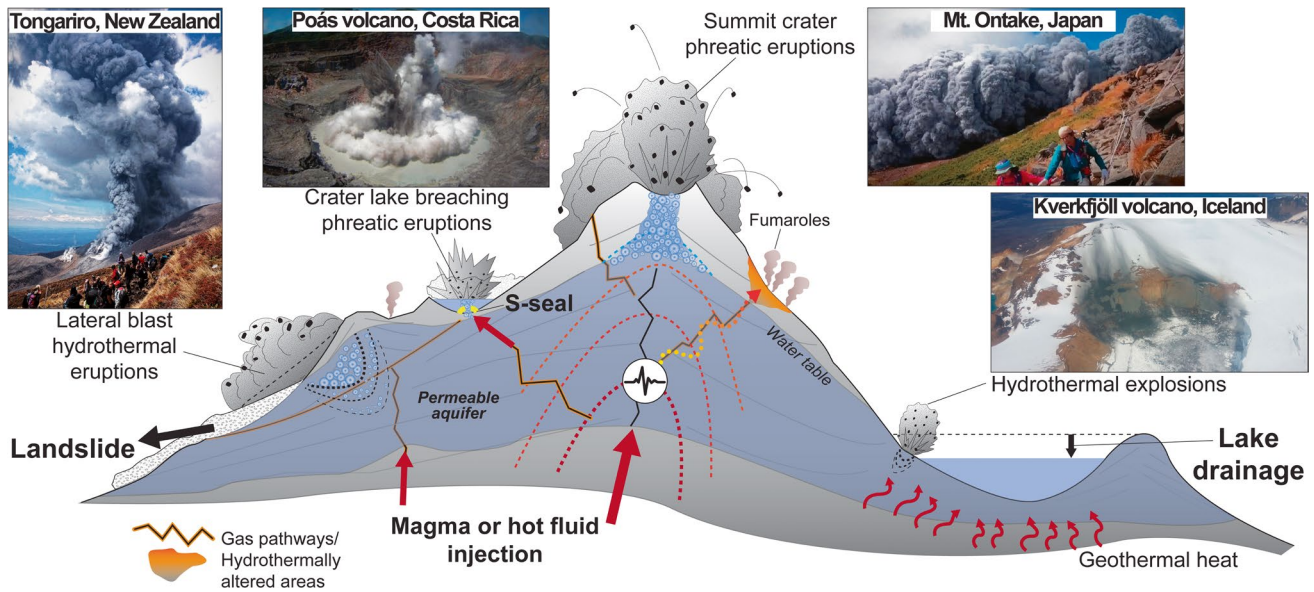


**Fig. 2** Conceptual sketch of typical phreatic and hydrothermal eruption types in volcanic and geothermal settings, showing potential trigger mechanisms (e.g., magma/fluid injection; landslide; sulphur sealing; lake drainage). Examples of respective eruption types from Te Maari/Tongariro 2012, Poás 2014, Mt. Ontake 2014, and Kverkfjöll/

Gengissig 2013, are shown. *Note:* the Te Maari eruption shown in the picture is the one from November, while the event of August occurred overnight. It can be noted how pyroclastic flow move within the scar left by the landslide triggering the August eruption

varying space and time scales (Harris et al. 2012; Heap and Kennedy 2016; Kanakiya et al. 2017; Roulleau et al. 2017; Kennedy et al. 2020; Cid et al. 2021).

At stratovolcanoes, systems with near-surface magma or lava domes (e.g. Merapi, Lascar, Turrialba, Sinabung, Vulcano), fluids are hosted within primary and reworked pyroclastic deposits, as well as in fractured lavas. The dynamic interaction of ascending magmatic gases with the existing aquifer (cold or hydrothermal water) yields acid-sulphate alteration that can reduce conduit or cap rock permeability by orders of magnitude over timescales of weeks to years (Gurioli et al. 2012; Sutawidjaja et al. 2013; Heap et al. 2019; Gaete et al. 2020; Mick et al. 2021). If lakes occupy active craters (e.g. Poás, Kawah Ijen, Ruapehu, Kusatsu-Shirane), they can act as traps for high temperature gases, allowing the formation of molten elemental sulphur (> 114 °C) within the aquifer (Christenson et al. 2017; Yamamoto et al. 2017). Because sulphur viscosity drastically increases above ~ 160 °C, pore sealing and consequent permeability loss can occur when temperature rises above this threshold value (Christenson et al. 2010; Sutawidjaja et al. 2013; Manville et al. 2015; Scolamacchia and Cronin 2016; Rouwet et al. 2021).

Large calderas and volcano-tectonic rift environments are situated within broad basins containing flat-lying ignimbrites, fractured lavas and volcanoclastic sediments (Morgan et al. 2009; Rowland and Simmons 2012; Kennedy et al. 2018). In these cases, pressurised hydrothermal reservoirs develop below clay caps formed by alteration of feldspar-rich tuffs, breccias and lavas during circulation of alkali chloride-rich fluids as

at, for example, Yellowstone, Waiotapu, Ebinokogen Ioyama, Domuyo, Valley of Desolation, Krafla (Mayer et al. 2017; Fowler et al. 2019; D'Elia et al. 2020; Eggertsson et al. 2020; Tajima et al. 2020). The presence of clay-rich and impermeable structures has been confirmed at such systems via geophysical exploration (e.g. magnetotelluric methods; Tajima et al. 2020; Tseng et al. 2020). In such data, hydrothermal seals appear as low resistivity layers overlying a relatively conductive domain corresponding to pressure sources and low-frequency earthquake swarms associated with the dynamics of the hydrothermal reservoir (Seki et al. 2015; Yoshimura et al. 2018; Mannen et al. 2019; Taussi et al. 2019). Clay, silica and zeolite precipitation within surficial fluvial and lacustrine sediments may also form localised to large-scale shallow impermeable layers (Morgan et al. 2009; Montanaro et al. 2016b; Fowler et al. 2019; D'Elia et al. 2020).

## Triggers

In all geological settings, sealing locally elevates pressure and increases explosive potential. Addition of gas volume/heat into aquifers from deeper magmatic or tectonic sources can rapidly accelerate local overpressurisation and enhance explosive potential (Fig. 2). Injection of magmatic fluids prior to phreatic and hydrothermal eruptions has been detected by geophysical, geochemical and petrological investigations (Table 1). Cyclical pressurisation and fracturing enhance circulation of hot fluids within shallow portions of the hydrothermal systems and may indicate a

greater instability and risk of eruptions (Christenson et al. 2010; Rouwet et al. 2014, 2021; Jolly et al. 2018; Heap et al. 2019; Kennedy et al. 2020; Moretti et al. 2020). Such cyclical unrest periods are observed at Whakaari/White Island where short explosive paroxysms alternate with periods of pressure-induced fracturing resulting in “failed eruptions” (Dempsey et al. 2020). Similar periods of pressure-induced fracturing, and associated seismic and deformation trends, have also been observed and defined at Vulcano where they have been termed “apparent heating” phases (Harris et al. 2012). Characteristic tremor and degassing signals indicate that such behaviour reflects the presence of imperfect seals that readily leak and accommodate deformation pulses following magmatic fluid injections as at, for example, Solfatara in Campi Flegrei (Chiodini et al. 2017; Moretti et al. 2018; Lima et al. 2021).

Another possible trigger of phreatic and hydrothermal eruptions could be large regional tectonic earthquakes disturbing the local stress regime, provided that the “appropriate” priming conditions are present (Lupi and Miller 2014; Seropian et al. 2021). It has been observed that modest, proximal earthquakes can cause an increase in near-vent permeability and trigger mild bursts of hydrothermal fluids (Hurwitz et al. 2014; Reed et al. 2021). Large events may cause rock fracturing to break aquifer seals or produce seismic waves that can perturb hydrothermal systems over different timescales and distances (Rouwet et al. 2019; González et al. 2021). For instance, the M7.6 Nicoya earthquake in Costa Rica in 2012 enhanced seismic and thermal activity at Irazú-Turrialba and Poás volcanoes (Lupi et al. 2014) and affected the eruptive activity in the following 2 to 5 years (de Moor et al. 2017; Salvage et al. 2018). Teleseismic waves from the M6.7 earthquake in Chile in 2014 triggered seismicity and a small phreatic eruption in the Tatun volcano group of Taiwan ~200 s afterwards (Lin 2017). A M5.9 earthquake located ~10 km NE of Whakaari/White Island occurred on November 24, 2019, about three weeks prior to the deadly eruption on December 19 (Ardid et al. 2022).

Other eruption triggers include (Fig. 2 and Table 1): i) mass movements causing unroofing of hydrothermal aquifers or burying of gas emission vents (Lube et al. 2014; Procter et al. 2014; Mayer et al. 2017; Isaia et al. 2021); ii) extensional fracturing (Ort et al. 2016); iii) groundwater-lake level changes (Montanaro et al. 2016b; Rott et al. 2019); iv) sudden precipitation events (Gaete et al. 2020); and v) rapid fracture/vein filling by calcite precipitation (Simpson et al. 2014).

### Lithological factors

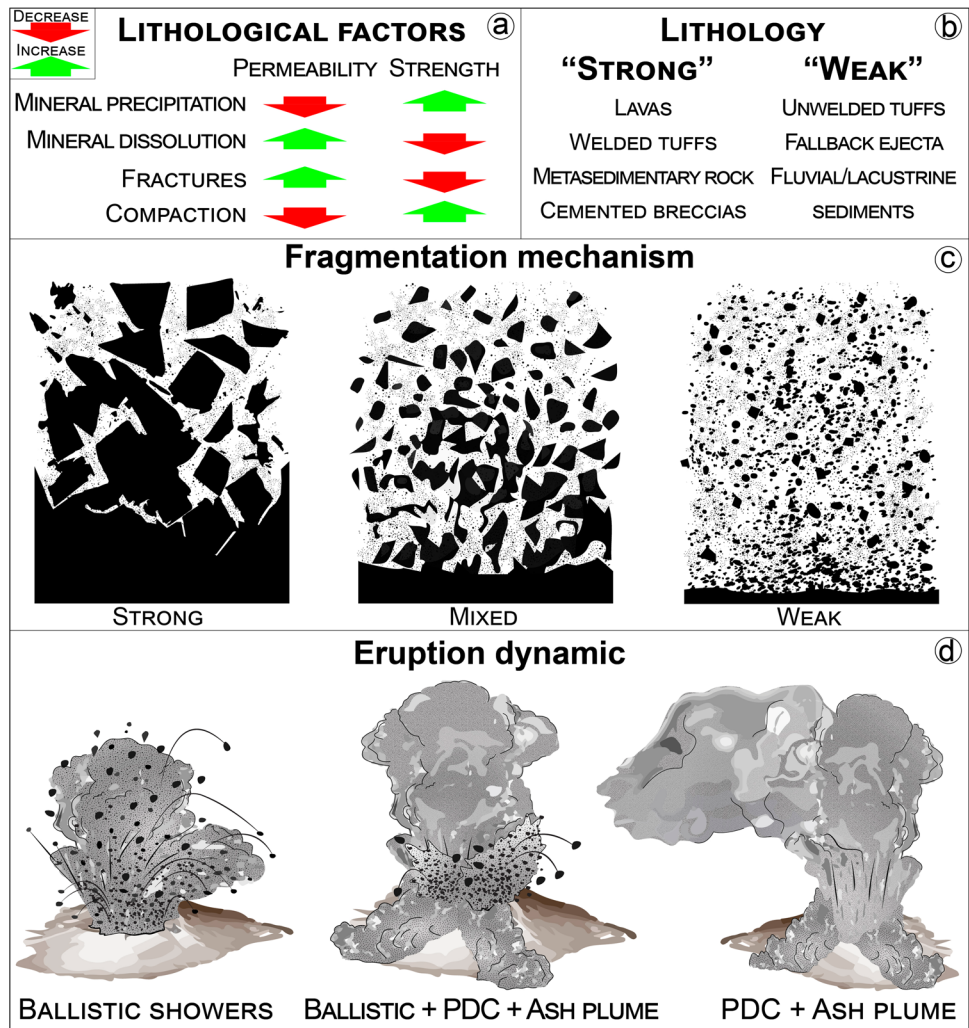
The eruptive mechanisms and processes of phreatic and hydrothermal events are strongly influenced by the properties of fragmented lithologies (Fig. 3; Breard et al. 2014; Graettinger et al. 2015; Valentine et al. 2015b; Pittari et al. 2016;

Geshi and Itoh 2018; Montanaro et al. 2020, 2021b; Graettinger and Bearden 2021). In particular, rock permeability determines whether expanding fluids may fragment the host rocks or escape via efficient outgassing, while rock strength can modulate fragmentation initiation, craterisation processes, and eruptive dynamics (Haug et al. 2013; Mayer et al. 2015; Montanaro et al. 2016a, c, 2021a). Both parameters can be influenced by alteration, fracturing and compaction processes (Fig. 3a). Mineral dissolution can increase permeability and reduce rock strength, whereas mineral precipitation has the opposite effect, favouring brittle behaviour (Pola et al. 2012; Mayer et al. 2016; Mordensky et al. 2019). Fractures tend to enhance permeability, favouring fluid circulation and eventual dissolution/precipitation, but might weaken host rocks, whereas compaction tends to close pores and fractures reducing permeability and increasing strength (Heap et al. 2015; Heap and Violay 2021).

Experiments, field studies and modelling (Taddeucci et al. 2013; Graettinger et al. 2015; Valentine et al. 2015a; Macorps et al. 2016; Montanaro et al. 2016a, 2021a; Tsunematsu et al. 2016; Strehlow et al. 2017; Rosi et al. 2018; Gallagher et al. 2020) reveal that fragmentation of fresh or altered “strong” lithologies requires significant mechanical energy to create intergranular fractures, thus reducing the efficiency of size-reduction processes and ash generation (Fig. 3b, c). Consequently, disruption of aquifers dominated by lithologies of high rock strength can result in relatively smaller deposit footprints, abundant blocks and low particle ejection velocities as inferred from eruption deposits at King’s Bowl and Vulcano (Fig. 3d; Hughes et al. 2018; Rosi et al. 2018). In contrast, fragmentation and/or disaggregation of weathered and degraded rocks, or poorly consolidated to unconsolidated “weak” lithologies requires little energy, and produces a significant amount of ash (Fig. 3b, c). Thus, eruptions that disrupt aquifers within lithologies of low rock strength result in more efficient craterisation and debris dispersion. That is, they are associated with relatively higher ejecta volumes, greater particle ejection velocities and larger ejecta footprints as at, for example, Turrialba, Whakaari/White Island, Kusatsu-Shirane, and Kverkfjöll/Gengisig (Fig. 3d, Table 1). Aquifers composed of a mixture of strong and weak lithologies are expected to produce a mixed spectrum of eruption types and hazards (Fig. 3c), as at, for example, Te Maari/Tongariro and Mt. Ontake (Table 1), or as inferred from eruption deposits at Lake Okaro and El Humazo (D’Elia et al. 2020; Montanaro et al. 2020). Lithological effects on eruption dynamics are masked by eruptions through lakes, which can produce vapour-debris mixtures such as cockscomb jets, base surges and eventual lake breaching as at, for instance, Poás and Ruapehu (Fig. 2; Kilgour et al. 2010; Manville et al. 2015).



**Fig. 3** Lithological factors and their implication for fragmentation and eruption dynamics. **a** Effect of mineral dissolution/precipitation, fractures and compaction over bulk permeability and strength of aquifer host rocks. **b** Example of essential strong and weak lithologies is also given. **c** Conceptual sketch of host rock fragmentation showing how strong lithologies are difficult to fragment, producing mainly coarse fragments. Conversely, fragmentation/dissaggregation of weak/unconsolidated lithologies is more efficient and produces larger proportions of fine ejecta. **d** Conceptual model of eruptive dynamics in relation to dominant lithologies within exploded aquifers. Eruptions involving dominantly strong lithologies produce ballistic showers and ash blasts, weak lithologies produce mainly surges and ash plumes, while mixed lithologies can produce both



### Forecasting

To date no phreatic or hydrothermal eruption has been successfully forecasted. This presents a significant challenge to volcano observatories and monitoring systems. Here we outline four recent notable advances that may aid in increasing our forecasting capabilities:

- Seismicity and/or tremor commonly occurs just prior to (e.g. Kawakatsu et al. 2000; Park et al. 2020) or associated with phreatic and hydrothermal eruptions (Maeda et al. 2015; Tajima et al. 2020). Such signals may reflect periods of pressurisation. At Whakaari/White Island, some of the phreatic and hydrothermal eruptions were preceded by tremor episodes during which seismic amplitude increased from 2 to 5 Hz (Chardot et al. 2015; Dempsey et al. 2020; Ardid et al. 2022). Seismic velocities and attenuation can also change preceding the eruptions (Mordret et al. 2010; Saade et al. 2019; Yates et al. 2019). Month to

year-long changes in seismic amplitude ratios prior to several eruptive events have indicated enhanced attenuation at shallow levels (Caudron et al. 2019). These seismic "signatures" may be sensitive monitors of both sudden gas influx and volatile accumulation due to sealing.

- On timescales of years, increases in radiant heat fluxes were observed prior to phreatic eruptions at Mt. Ontake and Ruapehu, possibly related to magmatic fluid-enhanced hydrothermal activity (Girona et al. 2021). Deformation signals can also occur, such as at Hakone, where InSAR and GNSS data revealed ground inflation starting in mid-2014 prior to a small hydrothermal eruption in June 2015 (Doke et al. 2018; Kobayashi et al. 2018; Mannen et al. 2019). Such anomalies require spatial resolutions of ~100 m if they are to be detected within the limits of our current remote sensing capability (Narita et al. 2020). A similar but subtle signal was detected in hindsight by stacking GNSS data prior to the 2014 Mt. Ontake eruption (Miyaoaka and Takagi 2016).

Conversely, more widespread deformation was observed prior to the 2017 Poás eruption, which involved magma (de Moor et al. 2019).

- Continuous gas monitoring provides significant insight into eruption “priming” processes at various timescales. Examples include: i) Poás, where SO<sub>2</sub> fluxes and MultiGAS SO<sub>2</sub>/CO<sub>2</sub> and H<sub>2</sub>S/SO<sub>2</sub> ratios distinguish periods of hydrothermal sealing (closed-system, SO<sub>2</sub> flux < 20 T/day, SO<sub>2</sub>/CO<sub>2</sub> < 0.1, H<sub>2</sub>S/SO<sub>2</sub> 1–5) from magmatic inputs (open-system, SO<sub>2</sub> fluxes > 50 T/day, SO<sub>2</sub>/CO<sub>2</sub> > 1, H<sub>2</sub>S/SO<sub>2</sub> near zero) on timescales of weeks to months (de Moor et al. 2019); ii) Rincón de la Vieja, where low concentrations of SO<sub>2</sub> and H<sub>2</sub>S are observed minutes prior to phreatic eruptions—likely due to a forming sulphur seal—while eruptive gases are characterised by large increases in SO<sub>2</sub> relative to H<sub>2</sub>S and CO<sub>2</sub> (Battaglia et al. 2019); and iii) Turrialba with peaks in CO<sub>2</sub>/SO<sub>2</sub> prior to eruptive phases in 2014 and 2015 signal magma injection that disrupted the overlying hydrothermal system, whereas the disappearance of H<sub>2</sub>S in emissions marked the transition from phreatic to phreatomagmatic activity (de Moor et al. 2016). The distinct degassing behaviour of these volcanoes highlights the challenge of identifying universal precursors to phreatic and hydrothermal eruptions.
- Several studies have utilised Bayesian tools to combine catalogued phreatic and hydrothermal eruptions (e.g. ballistics and pyroclastic deposit distributions) with monitoring data (seismic, gas emissions, deformation) to model multiple variables for probabilistic forecasting and hazard assessment (García-Aristizabal et al. 2013; Rouwet et al. 2014; Tonini et al. 2016; Strehlow et al. 2017; Christophersen et al. 2018). New monitoring data will enable better uncertainty assessment and statistical analyses to support more accurate risk analysis. A method of tremor analysis that uses machine learning has been used to scrutinise continuous seismic energy data to forecast eruptions at Whakaari/White Island (Dempsey et al. 2020). Patterns of events preceding past eruptions were used to classify 48-h-long windows of the seismic record. Patterns that could indicate pre-eruptive “boiling” instabilities in the aquifer were identified, and threshold values of seismic energy indicating higher probabilities of eruption were constructed for automatic recognition. Both these novel approaches hold significant promise.

## Perspectives

On the basis of our assessment, we identify five priority areas for research over the coming decade. These are:

1. *Unravelling the critical rates of fluid-rock interaction and related aquifer processes that prime hydrothermal systems for explosive failure:* The kinetics of mineral dissolution and precipitation determine *if* and *when* unstable conditions are reached within hydrothermal aquifers. New experimental, geochemical, mineralogical and numerical techniques capable of unravelling the spatial and temporal variability of aquifer sealing are needed. Models built on such knowledge will be pivotal in understanding the relative stability or instability degree of any given aquifer. The extensive recent research related to carbon storage could serve as a cornerstone in advancing experimental, analytical and model-based research (Kaszuba et al. 2013; Tonini et al. 2016; Vialle et al. 2018; Wu and Li 2020; Payton et al. 2022).
2. *Identification of areas with potential for future phreatic and hydrothermal eruptions:* Building extensive and new geological knowledge for areas with long-term hydrothermal activity, crater lake floors, histories of previous/ongoing eruptions and geothermal-system crises are pivotal to delineate cases in which eruptive events are likely to occur without obvious precursory signals. A challenging, but necessary, step will include the identification of potential sites at risk of disruption at relatively long-dormant (decades to centuries) volcanoes, where evidence of past eruptions is absent or not recognisable. New geophysical and remote sensing exploration methods for mapping of altered ground and delimiting covert hydrothermal aquifers might help in tackling this problem (Kruse 2012; Hübert et al. 2016; Gresse et al. 2017, 2021; Vaughan et al. 2020; Mishra et al. 2021; Rodriguez-gomez et al. 2021; Wang et al. 2021).
3. *Building new eruption forecasting tools and indicators over a range of timescales:* Currently, forecasting systems rely on data collected at different sampling frequencies and under different technical and field constraints. For instance the time resolution of continuous acquisition of seismic or deformation data, in contrast to sporadic or punctual gas and geochemical sampling. Real-time seismic amplitude monitoring (RSAM), displacement seismic amplitude ratio (DSAR), radiant heat flux and Multi-GAS datasets can provide remote and quasi-continuous, key information capable of indicating when a system becomes unstable (Caudron et al. 2021). Integrating these tools using a machine-learning approach can provide means to combine high frequency with sporadically collected data, and thus enable the weight of these parameters to objectively forecast an eruption likelihood. Such an approach requires numerical advances in order to transfer knowledge between systems and move from isolated case studies to globally applicable techniques.
4. *Development of broad, global approaches to statistical hazard estimation:* Current understanding of lithological influences on explosive energy partitioning allows us to estimate eruptive scenarios and hazards for a range of volcanic, geothermal and other lithological settings. Integrating large datasets involving a number of differ-

ent sites and using numerical and statistical modelling is needed to generalise and extend an approach based on probabilistic or event-tree type methods.

5. *Developing new hazard mitigation and communication strategies:* The sudden and unexpected nature of phreatic and hydrothermal eruptions demands that we develop rapid and automated warning tools. However, it will be challenging to understand the limits of such tools, and consider how best to transfer the alert information of an imminent eruption as quickly as possible, using plain language that the public can understand, and also remaining true to the inherent uncertainties in forecasting events (Fearnley et al. 2017; Fitzgerald et al. 2017; Yamada 2022). Ongoing strategies used, for example in Japan, foresee precise and dense monitoring of geothermal and fumarolic areas, where anomalies and crises are assessed in terms of seismicity, geodesy and geochemistry. Such dense monitoring allowed, for instance, to detect the unrest at Hakone, and to rapidly implement hazard mitigation measures (e.g., pre-established evacuation manual) that reduced the risk of having people exposed to the volcanic hazard (Mannen et al. 2018).

The last decade has shown great progress in our understanding of priming and triggering conditions of phreatic and hydrothermal eruptions, as well as on the characterisation and modelling of their eruptive processes. Such progress also enabled a better monitoring and analysis of seismic, geochemical and deformational “changes” in the volcanic and geothermal settings eventually preceding eruptive failures. However, inherent uncertainties in interpreting diverse and potentially contradictory signals may still lead to high rates of false “crises” and, thus potentially, “false alarms”. In the next decade comprehensive models of aquifer priming and explosive failure will build up on continuous progress through novel approaches and new technologies. Future advancement will enable for more accurate, quantitative forecasts that better communicate uncertainty and mitigate risks from such eruptions.

**Supplementary Information** The online version contains supplementary material available at <https://doi.org/10.1007/s00445-022-01571-7>.

**Acknowledgements** C.M. and B.S. acknowledge the Deutsche Forschungsgemeinschaft grants MO3508/1–1 and SCHE 1634/1–1. C.M., S.J.C. and B.S. also thank the NZ Ministry for Business, Innovation and Employment for funding support through the Transitioning Taranaki to a Volcanic Future Research Programme, UOAX1913. J.S. acknowledges support from an NSERC Discovery grant. J.M.dM. acknowledges support from the Costa Rican Ley Transitorio 8933 for volcanic hazard assessment. OVSICORI is gratefully acknowledged for providing the video footage of Rincón de la Vieja eruption. We thank Dr. Alison Graettinger, an anonymous reviewer, and the Editors Katharine V. Cashman and Andrew Harris for the useful comments that improved the paper.

**Author contributions** All authors contributed to the writing of the manuscript and the preparation of the figures.

**Funding** Open Access funding enabled and organized by Projekt DEAL.

**Open Access** This article is licensed under a Creative Commons Attribution 4.0 International License, which permits use, sharing, adaptation, distribution and reproduction in any medium or format, as long as you give appropriate credit to the original author(s) and the source, provide a link to the Creative Commons licence, and indicate if changes were made. The images or other third party material in this article are included in the article's Creative Commons licence, unless indicated otherwise in a credit line to the material. If material is not included in the article's Creative Commons licence and your intended use is not permitted by statutory regulation or exceeds the permitted use, you will need to obtain permission directly from the copyright holder. To view a copy of this licence, visit <http://creativecommons.org/licenses/by/4.0/>.

## References

- Alvarado GE, Mele D, Dellino P et al (2016) Are the ashes from the latest eruptions (2010–2016) at Turrialba volcano (Costa Rica) related to phreatic or phreatomagmatic events? *J Volcanol Geotherm Res* 327:407–415. <https://doi.org/10.1016/j.jvolgeores.2016.09.003>
- Ardid A, Dempsey D, Caudron C, Cronin SJ (2022) Seismic precursors to the Whakaari 2019 phreatic eruption are transferable to other eruptions and volcanoes. *Nat Commun* 13:1–9. <https://doi.org/10.1038/s41467-022-29681-y>
- Barberi F, Bertagnini A, Landi P, Principe C (1992) A review on phreatic eruptions and their precursors. *J Volcanol Geotherm Res* 52:231–246. [https://doi.org/10.1016/0377-0273\(92\)90046-G](https://doi.org/10.1016/0377-0273(92)90046-G)
- Battaglia A, de Moor JM, Aiuppa A et al (2019) Insights into the mechanisms of phreatic eruptions from continuous high frequency volcanic gas monitoring: Rincón de la Vieja Volcano, Costa Rica. *Front Earth Sci* 6:1–20. <https://doi.org/10.3389/feart.2018.00247>
- Breard ECP, Lube G, Cronin SJ et al (2014) Using the spatial distribution and lithology of ballistic blocks to interpret eruption sequence and dynamics: August 6 2012 Upper Te Maari eruption, New Zealand. *J Volcanol Geotherm Res* 286:373–386. <https://doi.org/10.1016/j.jvolgeores.2014.03.006>
- Browne PRL, Lawless JV (2001) Characteristics of hydrothermal eruptions, with examples from New Zealand and elsewhere. *Earth Sci Rev* 52:299–331. [https://doi.org/10.1016/S0012-8252\(00\)00030-1](https://doi.org/10.1016/S0012-8252(00)00030-1)
- Burton M, Hayer C, Miller C, Christenson B (2021) Insights into the 9 December 2019 eruption of Whakaari/White Island from analysis of TROPOMI SO<sub>2</sub> imagery. *Sci Adv* 7:1–12
- Caudron C, Girona T, Taisne B, Gunawan H (2019) Change in seismic attenuation as a long-term precursor of gas-driven eruptions. *Geology* 47:1–5. <https://doi.org/10.1130/G46107.1/4691758/g46107.pdf>
- Caudron C, Girona T, Jolly A, Christenson B, Savage MK, Carniel R, Lecocq T, Kennedy B, Lokmer I, Yates A, Hamling I, Park I, Kilgour G, Mazot A (2021) A quest for unrest in multiparameter observations at Whakaari/White Island volcano, New Zealand 2007–2018. *Earth, Planets Sp* 73. <https://doi.org/10.1186/s40623-021-01506-0>
- Chardot L, Jolly AD, Kennedy BM et al (2015) Using volcanic tremor for eruption forecasting at White Island volcano (Whakaari), New Zealand. *J Volcanol Geotherm Res* 302:11–23

- Chiodini G, Cioni R, Marini L, Panichi C (1995) Origin of the fumarolic fluids of Vulcano Island, Italy and implications for volcanic surveillance. *Bull Volcanol* 57:99–110
- Chiodini G, Selva J, Del Pezzo E et al (2017) Clues on the origin of post-2000 earthquakes at Campi Flegrei caldera (Italy). *Sci Rep* 7:1–10. <https://doi.org/10.1038/s41598-017-04845-9>
- Christenson BW, Reyes AG, Young R et al (2010) Cyclic processes and factors leading to phreatic eruption events: Insights from the 25 September 2007 eruption through Ruapehu Crater Lake, New Zealand. *J Volcanol Geotherm Res* 191:15–32. <https://doi.org/10.1016/j.jvolgeores.2010.01.008>
- Christenson BW, White S, Britten K, Scott BJ (2017) Hydrological evolution and chemical structure of a hyper-acidic spring-lake system on Whakaari/White Island, NZ. *J Volcanol Geotherm Res* 346:180–211. <https://doi.org/10.1016/j.jvolgeores.2017.06.017>
- Christophersen A, Deligne NI, Hanea AM et al (2018) Bayesian Network Modeling and Expert Elicitation for Probabilistic Eruption Forecasting: Pilot Study for Whakaari/White Island, New Zealand. *Front Earth Sci* 6:1–23. <https://doi.org/10.3389/feart.2018.00211>
- Cid HE, Carrasco-Núñez G, Manea VC, Vega S, Castaño V (2021) The role of microporosity on the permeability of volcanic-hosted geothermal reservoirs: a case study from Los Humeros, Mexico. *Geothermics* 90. <https://doi.org/10.1016/j.geothermics.2020.102020>
- D'Elia L, Páez G, Hernando IR et al (2020) Hydrothermal eruptions at El Humazo, Domuyo geothermal field, Argentina: Insights into the eruptive dynamics and controls. *J Volcanol Geotherm Res* 393:106786. <https://doi.org/10.1016/j.jvolgeores.2020.106786>
- de Moor JM, Aiuppa A, Avarad G et al (2016) Turmoil at Turrialba Volcano (Costa Rica): Degassing and eruptive processes inferred from high-frequency gas monitoring. *J Geophys Res Solid Earth* 121:3782–3803. <https://doi.org/10.1002/2016JB013150>
- de Moor JM, Kern C, Avarad G, Muller C, Aiuppa A, Saballos A, Ibarra M, LaFemina P, Protti M, Fischer TP (2017) A new sulfur and carbon degassing inventory for the Southern Central American Volcanic Arc: The importance of accurate time-series data sets and possible tectonic processes responsible for temporal variations in arc-scale volatile emissions. *Geochem Geophys Geosystems* 18(12):4437–4468. <https://doi.org/10.1002/2017GC007141>
- de Moor JM, Stix J, Avarad G et al (2019) Insights on Hydrothermal-Magmatic Interactions and Eruptive Processes at Poás Volcano (Costa Rica) From High-Frequency Gas Monitoring and Drone Measurements. *Geophys Res Lett* 46:1293–1302. <https://doi.org/10.1029/2018GL080301>
- Dempsey DE, Cronin SJ, Mei S, Kempa-Liehr AW (2020) Automatic precursor recognition and real-time forecasting of sudden explosive volcanic eruptions at Whakaari, New Zealand. *Nat Commun* 11:1–8. <https://doi.org/10.1038/s41467-020-17375-2>
- DeVitre CL, Gazel E, Allison CM et al (2019) Multi-stage chaotic magma mixing at Turrialba volcano. *J Volcanol Geotherm Res* 381:330–346. <https://doi.org/10.1016/j.jvolgeores.2019.06.011>
- Doke R, Harada M, Mannen K, Itadera K, Takenaka J (2018) InSAR analysis for detecting the route of hydrothermal fluid to the surface during the 2015 phreatic eruption of Hakone Volcano, Japan. *Earth, Planets Sp* 70. <https://doi.org/10.1186/s40623-018-0834-4>
- Eggertsson GH, Lavallée Y, Kendrick JE, Markússon SH (2020) Improving fluid flow in geothermal reservoirs by thermal and mechanical stimulation: The case of Krafla volcano, Iceland. *J Volcanol Geotherm Res* 391:106351. <https://doi.org/10.1016/j.jvolgeores.2018.04.008>
- Erfurt-cooper P (ed) (2014) *Volcanic Tourist Destinations*. Geohertag. Springer, Berlin, Heidelberg. <https://doi.org/10.1007/978-3-642-16191-9>
- Fearnley C, Winson AEG, Pallister J, Tilling R (2017) *Volcano Crisis Communication: Challenges and Solutions in the 21st Century*. In: Fearnley CJ, Bird DK, Haynes K, McGuire, WJ, Jolly G (eds) *Observing the Volcano World*. Advances in Volcanology. Springer, Cham, pp 3–21. [https://doi.org/10.1007/11157\\_2017](https://doi.org/10.1007/11157_2017)
- Fitzgerald RH, Kennedy BM, Wilson TM et al (2017) *The Communication and Risk Management of Volcanic Ballistic Hazards*. Advances in Volcanology. Springer, Berlin Heidelberg, Berlin, Heidelberg, pp 1–27
- Fowler APG, Tan C, Cino C et al (2019) Vapor-driven sublacustrine vents in Yellowstone Lake, Wyoming, USA. *Geology* 47:223–226. <https://doi.org/10.1130/G45577.1>
- Fullard LA, Lynch TA (2012) On the Initiation of a Hydrothermal Eruption Using the Shock-Tube Model. *Transp Porous Media* 94:19–46. <https://doi.org/10.1007/s11242-012-9986-z>
- Gaete A, Walter TR, Bredemeyer S et al (2020) Processes culminating in the 2015 phreatic explosion at Lascar volcano, Chile, evidenced by multiparametric data. *Nat Hazards Earth Syst Sci* 20:377–397. <https://doi.org/10.5194/nhess-20-377-2020>
- Gallagher A, Montanaro C, Cronin SJ et al (2020) Hydrothermal eruption dynamics reflecting vertical variations in host rock geology and geothermal alteration, Champagne Pool, Wai-o-tapu, New Zealand *Bull Volcanol* 82:19. <https://doi.org/10.1007/s00445-020-01414-3>
- Galland O, Gisler GR, Haug OT (2014) Morphology and dynamics of explosive vents through cohesive rock formations. *J Geophys Res Solid Earth* 119:4708–4728. <https://doi.org/10.1002/2014JB011050>
- Garcia-Aristizabal A, Selva J, Fujita E (2013) Integration of stochastic models for long-term eruption forecasting into a Bayesian event tree scheme: A basis method to estimate the probability of volcanic unrest. *Bull Volcanol* 75:1–13. <https://doi.org/10.1007/s00445-013-0689-2>
- Geshi N, Itoh J (2018) Pyroclastic density currents associated with the 2015 phreatomagmatic eruption of the Kuchinoerabujima volcano. *Earth, Planets Sp* 70. <https://doi.org/10.1186/s40623-018-0881-x>
- Girona T, Realmuto V, Lundgren P (2021) Large-scale thermal unrest of volcanoes for years prior to eruption. *Nat Geosci* 14:238–241. <https://doi.org/10.1038/s41561-021-00705-4>
- González G, Fujita E, Shibazaki B et al (2021) Increment in the volcanic unrest and number of eruptions after the 2012 large earthquakes sequence in Central America. *Sci Rep* 11:1–11. <https://doi.org/10.1038/s41598-021-01725-1>
- Graettinger AH, Bearden AT (2021) Lateral migration of explosive hazards during maar eruptions constrained from crater shapes. *J Appl Volcanol* 10:1–14. <https://doi.org/10.1186/s13617-021-00103-w>
- Graettinger AH, Valentine GA, Sonder I (2015) Circum-crater variability of deposits from discrete, laterally and vertically migrating volcanic explosions: Experimental evidence and field implications. *J Volcanol Geotherm Res* 308:61–69. <https://doi.org/10.1016/j.jvolgeores.2015.10.019>
- Gresse M, Vandemeulebrouck J, Byrdina S et al (2017) Three-Dimensional Electrical Resistivity Tomography of the Solfatara Crater (Italy): Implication for the Multiphase Flow Structure of the Shallow Hydrothermal System. *J Geophys Res Solid Earth* 122:8749–8768. <https://doi.org/10.1002/2017JB014389>
- Gresse M, Uyeshima M, Koyama T et al (2021) Hydrothermal and Magmatic System of a Volcanic Island Inferred From Magnetotellurics, Seismicity, Self-potential, and Thermal Image: An Example of Miyakejima (Japan). *J Geophys Res Solid Earth* 126:1–24. <https://doi.org/10.1029/2021JB022034>
- Gurioli L, Zanella E, Gioncada A, Sbrana A (2012) The historic magmatic-hydrothermal eruption of the Breccia di Commenda, Vulcano, Italy. *Bull Volcanol* 74:1235–1254. <https://doi.org/10.1007/s00445-012-0590-4>

- Hamling IJ (2017) Crater Lake Controls on Volcano Stability: Insights From White Island, New Zealand. *Geophys Res Lett* 44:11,311–11,319. <https://doi.org/10.1002/2017GL075572>
- Harris A, Alparone S, Bonforte A et al (2012) Vent temperature trends at the Vulcano Fossa fumarole field: The role of permeability. *Bull Volcanol* 74:1293–1311. <https://doi.org/10.1007/s00445-012-0593-1>
- Haug ØT, Galland O, Gislér GR (2013) Experimental modelling of fragmentation applied to volcanic explosions. *Earth Planet Sci Lett* 384:188–197. <https://doi.org/10.1016/j.epsl.2013.10.004>
- Heap MJ, Kennedy BM (2016) Exploring the scale-dependent permeability of fractured andesite. *Earth Planet Sci Lett* 447:139–150. <https://doi.org/10.1016/j.epsl.2016.05.004>
- Heap MJ, Brantut N, Baud P, Meredith PG (2015) Time-dependent compaction band formation in sandstone. *J Geophys Res Solid Earth* 120:4808–4830. <https://doi.org/10.1002/2015JB012022>. Received
- Heap MJ, Troll VR, Kushnir ARL et al (2019) Hydrothermal alteration of andesitic lava domes can lead to explosive volcanic behaviour. *Nat Commun* 10:1–10. <https://doi.org/10.1038/s41467-019-13102-8>
- Heap MJ, Violay MES (2021) The mechanical behaviour and failure modes of volcanic rocks: a review. *Bull Volcanol* 83. <https://doi.org/10.1007/s00445-021-01447-2>
- Hübert J, Lee BM, Liu L et al (2016) Three-dimensional imaging of a Ag-Au-rich epithermal system in British Columbia, Canada, using airborne z-axis tipper electromagnetic and ground-based magnetotelluric data. *Geophysics* 81:B1–B12. <https://doi.org/10.1190/GEO2015-0230.1>
- Hughes SS, Kobs Nawotniak SE, Sears DWG et al (2018) Phreatic explosions during basaltic fissure eruptions: Kings Bowl lava field, Snake River Plain, USA. *J Volcanol Geotherm Res* 351:89–104. <https://doi.org/10.1016/j.jvolgeores.2018.01.001>
- Hurst T, Jolly AD, Sherburn S (2014) Precursory characteristics of the seismicity before the 6 August 2012 eruption of Tongariro volcano, North Island, New Zealand. *J Volcanol Geotherm Res.* <https://doi.org/10.1016/j.jvolgeores.2014.03.004>
- Hurwitz S, Sohn RARA, Luttrell K, Manga M (2014) Triggering and modulation of geyser eruptions in Yellowstone National Park by earthquakes, earth tides, and weather. *J Geophys Res Solid Earth* 119:1718–1737. <https://doi.org/10.1002/2013JB010803>. Received
- Hurwitz S, Clor LE, McCleskey RB et al (2016) Dissolved gases in hydrothermal (phreatic) and geyser eruptions at Yellowstone National Park, USA. *Geology* 44(G37478):1. <https://doi.org/10.1130/G37478.1>
- Isaia R, Giulia M, Giuseppe D, Natale J, Tramparulo FDA, Troiano A, Vitale S, (2021) Volcano-Tectonic Setting of the Pisciarelli Fumarole Field, Campi Flegrei Caldera, Southern Italy: insights into fluid circulation patterns and hazard scenarios. *Tectonics* 1–22. <https://doi.org/10.1029/2020TC006227>
- Jolly AD, Jousset P, Lyons JJ et al (2014) Seismo-acoustic evidence for an avalanche driven phreatic eruption through a beheaded hydrothermal system: An example from the 2012 Tongariro eruption. *J Volcanol Geotherm Res* 286:317–330. <https://doi.org/10.1016/j.jvolgeores.2014.04.007>
- Jolly A, Lokmer I, Christenson B, Thun J (2018) Relating gas ascent to eruption triggering for the April 27, 2016, White Island (Whakaari), New Zealand eruption sequence. *Earth, Planets Sp* 70:1–15. <https://doi.org/10.1186/s40623-018-0948-8>
- Kanakiya S, Adam L, Esteban L et al (2017) Dissolution and secondary mineral precipitation in basalts due to reactions with carbonic acid. *J Geophys Res Solid Earth* 122:4312–4327. <https://doi.org/10.1002/2017JB014019>
- Kaneko T, Maeno F, Nakada S (2016) 2014 Mount Ontake eruption: characteristics of the phreatic eruption as inferred from aerial observations. *Earth, Planets Sp* 68:1–11. <https://doi.org/10.1186/s40623-016-0452-y>
- Kaszuba J, Yardley B, Andreani M (2013) Experimental perspectives of mineral dissolution and precipitation due to carbon dioxide-water-rock interactions. *Rev Mineral Geochemistry* 77:153–188. <https://doi.org/10.2138/rmg.2013.77.5>
- Kato A, Terakawa T, Yamanaka Y et al (2015) Preparatory and precursory processes leading up to the 2014 phreatic eruption of Mount Ontake, Japan. *Earth, Planets Sp* 67:111. <https://doi.org/10.1186/s40623-015-0288-x>
- Kawakatsu H, Kaneshima S, Matsubayashi H et al (2000) Aso94: Aso seismic observation with broadband instruments. *J Volcanol Geotherm Res* 101:129–154. [https://doi.org/10.1016/S0377-0273\(00\)00166-9](https://doi.org/10.1016/S0377-0273(00)00166-9)
- Kennedy BM, Holohan EP, Stix J et al (2018) Magma plumbing beneath collapse caldera volcanic systems. *Earth-Science Rev* 177:404–424. <https://doi.org/10.1016/j.earscirev.2017.12.002>
- Kennedy BM, Farquhar A, Hilderman R et al (2020) Pressure Controlled Permeability in a Conduit Filled with Fractured Hydrothermal Breccia Reconstructed from Ballistics from Whakaari (White Island), New Zealand. *Geosciences* 10:1–19. <https://doi.org/10.3390/geosciences10040138>
- Kilgour G, Manville V, Della PF et al (2010) The 25 September 2007 eruption of Mount Ruapehu, New Zealand: Directed ballistics, surtseyan jets, and ice-slurry lahars. *J Volcanol Geotherm Res* 191:1–14. <https://doi.org/10.1016/j.jvolgeores.2009.10.015>
- Kilgour G, Gates S, Kennedy B et al (2019) Phreatic eruption dynamics derived from deposit analysis: a case study from a small, phreatic eruption from Whakāri/White Island, New Zealand. *Earth, Planets Sp* 71:21. <https://doi.org/10.1186/s40623-019-1008-8>
- Kobayashi T, Morishita Y, Munekane H (2018) First detection of precursory ground inflation of a small phreatic eruption by InSAR. *Earth Planet Sci Lett* 491:244–254. <https://doi.org/10.1016/j.epsl.2018.03.041>
- Kruse FA (2012) Mapping surface mineralogy using imaging spectrometry. *Geomorphology* 137:41–56. <https://doi.org/10.1016/j.geomorph.2010.09.032>
- Lima A, Bodnar RJ, De Vivo B, Spera FJ, Belkin HE (2021) Interpretation of recent unrest events (Bradyseism) at Campi Flegrei, Napoli (Italy): comparison of models based on cyclical hydrothermal events versus shallow magmatic intrusive events. *Geo-fluids*. <https://doi.org/10.1155/2021/2000255>
- Lin CH (2017) Probable dynamic triggering of phreatic eruption in the Tatun volcano group of Taiwan. *J Asian Earth Sci* 149:78–85. <https://doi.org/10.1016/j.jseas.2017.01.023>
- Lube G, Breard ECP, Cronin SJ, Procter JN, Brenna M, Moebis A, Pardo N, Stewart RB, Jolly A, Fournier N (2014) Dynamics of surges generated by hydrothermal blasts during the 6 August 2012 Te Maari eruption, Mt. Tongariro, New Zealand. *J Volcanol Geotherm Res.* <https://doi.org/10.1016/j.jvolgeores.2014.05.010>
- Lupi M, Miller SA (2014) Short-lived tectonic switch mechanism for long-term pulses of volcanic activity after mega-thrust earthquakes. *Solid Earth* 5:13–24. <https://doi.org/10.5194/se-5-13-2014>
- Lupi M, Fuchs F, Pacheco JF (2014) Fault reactivation due to the M7.6 Nicoya earthquake at the Turrialba-Irazu volcanic complex, Costa Rica: Effects of dynamic stress triggering. *Geophys Res Lett* 41:4142–4148. <https://doi.org/10.1002/2014GL059942>
- Macorps É, Graettinger AH, Valentine GA et al (2016) The effects of the host-substrate properties on maar-diatreme volcanoes: experimental evidence. *Bull Volcanol* 78:1–12. <https://doi.org/10.1007/s00445-016-1013-8>
- Maeda Y, Kumagai H, Lacson R et al (2015) A phreatic explosion model inferred from a very long period seismic event at Mayon Volcano, Philippines. *J Geophys Res Solid Earth* 120:226–242. <https://doi.org/10.1002/2014JB011440>

- Maeno F, Nakada S, Oikawa T, Yoshimoto M, Komori J, Ishizuka Y, Takeshita Y, Shimano T, Kaneko T, Nagai M (2016) Reconstruction of a phreatic eruption on 27 September 2014 at Ontake volcano, central Japan, based on proximal pyroclastic density current and fallout deposits. *Earth, Planets Sp* 68. <https://doi.org/10.1186/s40623-016-0449-6>
- Mannen K, Yukutake Y, Kikugawa G, Harada M, Itadera K, Takenaka J (2018) Chronology of the 2015 eruption of Hakone volcano, Japan: geological background, mechanism of volcanic unrest and disaster mitigation measures during the crisis. *Earth, Planets Sp* 70. <https://doi.org/10.1186/s40623-018-0844-2>
- Mannen K, Tanada T, Jomori A, Akatsuka T, Kikugawa G, Fukazawa Y, Yamashita H, Fujimoto K (2019) Source constraints for the 2015 phreatic eruption of Hakone volcano, Japan, based on geological analysis and resistivity structure. *Earth, Planets Sp* 71. <https://doi.org/10.1186/s40623-019-1116-5>
- Manville V, Rouwet D, Morrissey MM (2015) Mechanisms of crater lake breaching eruptions. In: *Volcanic Lakes*. 73–91. <https://doi.org/10.1007/978-3-642-36833-2>
- Mastin LG (1995) Thermodynamics of gas and steam-blast eruptions. *Bull Volcanol* 57:85–98. <https://doi.org/10.1007/BF00301399>
- Matsunaga Y, Kanda W, Takakura S, Koyama T, Saito Z, Seki K, Suzuki A, Kishita T, Kinoshita Y, Ogawa Y (2020) Magmatic hydrothermal system inferred from the resistivity structure of Kusatsu-Shirane Volcano. *J Volcanol Geotherm Res* 390:106742. <https://doi.org/10.1016/j.jvolgeoes.2019.106742>
- Mayer K, Scheu B, Gilg HA et al (2015) Experimental constraints on phreatic eruption processes at Whakaari (White Island volcano). *J Volcanol Geotherm Res* 302:150–162. <https://doi.org/10.1016/j.jvolgeoes.2015.06.014>
- Mayer K, Scheu B, Montanaro C et al (2016) Hydrothermal alteration of surficial rocks at Solfatara (Campi Flegrei): Petrophysical properties and implications for phreatic eruption processes. *J Volcanol Geotherm Res* 320:128–143. <https://doi.org/10.1016/j.jvolgeoes.2016.04.020>
- Mayer K, Scheu B, Yilmaz TI et al (2017) Phreatic activity and hydrothermal alteration in the Valley of Desolation, Dominica. *Lesser Antilles Bull Volcanol* 79:19. <https://doi.org/10.1007/s00445-017-1166-0>
- Mick E, Stix J, de Moor JM, Avard G (2021) Hydrothermal alteration and sealing at Turrialba volcano, Costa Rica, as a mechanism for phreatic eruption triggering. *J Volcanol Geotherm Res* 416:1–14. <https://doi.org/10.1016/j.jvolgeoes.2021.107297>
- Mishra G, Govil H, Srivastava PK (2021) Identification of malachite and alteration minerals using airborne AVIRIS-NG hyperspectral data. *Quat Sci Adv* 4:100036. <https://doi.org/10.1016/j.qsa.2021.100036>
- Miyaoka K, Takagi A (2016) Detection of crustal deformation prior to the 2014 Mt. Ontake eruption by the stacking method. *Earth, Planets Sp* 68. <https://doi.org/10.1186/s40623-016-0439-8>
- Montanaro C, Scheu B, Cronin SJ et al (2016) Experimental estimates of the energy budget of hydrothermal eruptions; application to 2012 Upper Te Maari eruption, New Zealand. *Earth Planet Sci Lett* 452:281–294. <https://doi.org/10.1016/j.epsl.2016.07.052>
- Montanaro C, Scheu B, Gudmundsson MT et al (2016) Multidisciplinary constraints of hydrothermal explosions based on the 2013 Gengissig lake events, Kverkfjöll volcano, Iceland. *Earth Planet Sci Lett* 434:308–319. <https://doi.org/10.1016/j.epsl.2015.11.043>
- Montanaro C, Scheu B, Mayer K et al (2016) Experimental investigations on the explosivity of steam-driven eruptions: a case study of Solfatara volcano (Campi Flegrei). *J Geophys Res Solid Earth* 121:7996–8014. <https://doi.org/10.1002/2016JB013273>
- Montanaro C, Cronin SJ, Scheu B et al (2021) Host Rock Variability Powers the Diversity of Steam-Driven Eruptions. *Geophys Res Lett* 48:1–11. <https://doi.org/10.1029/2020gl089025>
- Montanaro C, Mortensen AK, Weisenberger TB et al (2021) Stratigraphic reconstruction of the Viti breccia at Krafla volcano (Iceland): Insights into pre-eruptive conditions priming eruptions in geothermal areas. *Bull Volcanol* 83:1–27. <https://doi.org/10.1007/s00445-021-01502-y>
- Montanaro C, Cronin S, Scheu B, Kennedy B, Scott B (2020) Complex crater fields formed by steam-driven eruptions: Lake Okaro, New Zealand. *GSA Bull* 132:1914–1930. <https://doi.org/10.1130/b35276.1>
- Mordensky SP, Heap MJ, Kennedy BM et al (2019) Influence of alteration on the mechanical behaviour and failure mode of andesite: implications for shallow seismicity and volcano monitoring. *Bull Volcanol* 44:13. <https://doi.org/10.1007/s00445-019-1306-9>
- Mordret A, Jolly AD, Duputel Z, Fournier N (2010) Monitoring of phreatic eruptions using Interferometry on Retrieved Cross-Correlation Function from Ambient Seismic Noise: Results from Mt. Ruapehu, New Zealand. *J Volcanol Geotherm Res* 191:46–59. <https://doi.org/10.1016/j.jvolgeoes.2010.01.010>
- Moretti R, Troise C, Sarno F, De Natale G (2018) Caldera unrest driven by CO<sub>2</sub>-induced drying of the deep hydrothermal system. *Sci Rep* 8:1–11. <https://doi.org/10.1038/s41598-018-26610-2>
- Moretti R, Komorowski JC, Ucciani G et al (2020) The 2018 unrest phase at La Soufrière of Guadeloupe (French West Indies) andesitic volcano: Scrutiny of a failed but prodromal phreatic eruption. *J Volcanol Geotherm Res* 393:106769. <https://doi.org/10.1016/j.jvolgeoes.2020.106769>
- Morgan LA, Shanks WCP, Pierce KL (2009) Hydrothermal processes above the Yellowstone magma chamber: large hydrothermal systems and large hydrothermal explosions. *Geol Soc Am Spec Pap* 459:1–95. [https://doi.org/10.1130/2009.2459\(01\)](https://doi.org/10.1130/2009.2459(01))
- Narita S, Ozawa T, Aoki Y, Shimada M, Furuya M, Takada Y, Murakami M (2020) Precursory ground deformation of the 2018 phreatic eruption on Iwo-Yama volcano, revealed by four-dimensional joint analysis of airborne and spaceborne InSAR. *Earth, Planets Sp* 72. <https://doi.org/10.1186/s40623-020-01280-5>
- Ohba T, Taniguchi H, Miyamoto T et al (2007) Mud plumbing system of an isolated phreatic eruption at Akita Yakeyama volcano, northern Honshu, Japan. *J Volcanol Geotherm Res* 161:35–46. <https://doi.org/10.1016/j.jvolgeoes.2006.11.001>
- Oikawa T, Yoshimoto M, Nakada S et al (2016) Reconstruction of the 2014 eruption sequence of Ontake Volcano from recorded images and interviews the Phreatic Eruption of Mt. Ontake Volcano in 2014 5. *Volcanology. Earth, Planets Sp* 68:1–13. <https://doi.org/10.1186/s40623-016-0458-5>
- Ort MH, Di Muro A, Michon L, Bachèlery P (2016) Explosive eruptions from the interaction of magmatic and hydrothermal systems during flank extension: the Bellecombe Tephra of Piton de La Fournaise (La Réunion Island). *Bull Volcanol* 78:1–14. <https://doi.org/10.1007/s00445-015-0998-8>
- Pardo N, Cronin SJ, Németh K et al (2014) Perils in distinguishing phreatic from phreatomagmatic ash; insights into the eruption mechanisms of the 6 August 2012 Mt. Tongariro eruption, New Zealand. *J Volcanol Geotherm Res* 286:397–414
- Park I, Jolly A, Lokmer I, Kennedy B (2020) Classification of long-term very long period (VLP) volcanic earthquakes at Whakaari/White Island volcano, New Zealand. *Earth, Planets Sp* 72. <https://doi.org/10.1186/s40623-020-01224-z>
- Payton RL, Sun Y, Chiarella D, Kingdon A (2022) Pore Scale Numerical Modelling of Geological Carbon Storage Through Mineral Trapping Using True Pore Geometries. *Transp Porous Media*. <https://doi.org/10.1007/s11242-021-01741-9>
- Pittari A, Briggs RM, Bowyer DA (2016) Subsurface geology, ancient hydrothermal systems and crater excavation processes beneath Lake Rotomahana: Evidence from lithic clasts of the

- 1886 AD Rotomahana Pyroclastics. *J Volcanol Geotherm Res* 314:110–125. <https://doi.org/10.1016/j.jvolgeores.2015.10.009>
- Pola A, Crosta G, Fusi N et al (2012) Influence of alteration on physical properties of volcanic rocks. *Tectonophysics* 566–567:67–86. <https://doi.org/10.1016/j.tecto.2012.07.017>
- Procter JN, Cronin SJ, Zernack a. V., et al (2014) Debris flow evolution and the activation of an explosive hydrothermal system; Te Maari, Tongariro, New Zealand. *J Volcanol Geotherm Res* 286:303–316. <https://doi.org/10.1016/j.jvolgeores.2014.07.006>
- Raue H (2004) A new model for the fracture energy budget of phreatomagmatic explosions. *J Volcanol Geotherm Res* 129:99–108. [https://doi.org/10.1016/S0377-0273\(03\)00234-8](https://doi.org/10.1016/S0377-0273(03)00234-8)
- Reed MH, Munoz-Saez C, Hajimirza S et al (2021) The 2018 reawakening and eruption dynamics of Steamboat Geyser, the world's tallest active geyser. *Proc Natl Acad Sci* 118:e2020943118. <https://doi.org/10.1073/pnas.2020943118>
- Rodriguez-gomez C, Kereszturi G, Reeves R et al (2021) Geothermics Lithological mapping of Waitapu Geothermal Field (New Zealand) using hyperspectral and thermal remote sensing and ground exploration techniques. *Geothermics* 96:1–15
- Rosi M, Di TF, Pistolesi M et al (2018) Dynamics of shallow hydrothermal eruptions: new insights from Vulcano's Breccia di Commenda eruption. *Bull Volcanol* 80:28. <https://doi.org/10.1007/s00445-018-1252-y>
- Rott S, Scheu B, Montanaro C et al (2019) Hydrothermal eruptions at unstable crater lakes: Insights from the Boiling Lake, Dominica, Lesser Antilles. *J Volcanol Geotherm Res* 381:101–118. <https://doi.org/10.1016/j.jvolgeores.2019.05.020>
- Rouilleau E, Bravo F, Pinti DL et al (2017) Structural controls on fluid circulation at the Cavihue-Copahue Volcanic Complex (CCVC) geothermal area (Chile-Argentina), revealed by soil CO<sub>2</sub> and temperature, self-potential, and helium isotopes. *J Volcanol Geotherm Res* 341:104–118. <https://doi.org/10.1016/j.jvolgeores.2017.05.010>
- Rouwet D, Sandri L, Marzocchi W et al (2014) Recognizing and tracking volcanic hazards related to non-magmatic unrest: A review. *J Appl Volcanol* 3:1–17. <https://doi.org/10.1186/s13617-014-0017-3>
- Rouwet D, Mora-Amador R, Ramirez C et al (2021) Response of a hydrothermal system to escalating phreatic unrest: the case of Turrialba and Irazú in Costa Rica (2007–2012). *Earth, Planets Sp* 73:1–26. <https://doi.org/10.1186/s40623-021-01471-8>
- Rouwet D, Hidalgo S, Joseph EP, González-Ilama G (2019) Fluid Geochemistry and Volcanic Unrest: dissolving the Haze in Time and Space. In: Gottsmann J, Neuberg J, Scheu B (eds) *Volcanic unrest. Advances in Volcanology*. Springer, Cham. [https://doi.org/10.1007/11157\\_2017\\_12](https://doi.org/10.1007/11157_2017_12)
- Rowland JV, Simmons SF (2012) Hydrologic, magmatic, and tectonic controls on hydrothermal flow, Taupo Volcanic Zone, New Zealand: implications for the formation of epithermal vein deposits. *Econ Geol* 107:427–457. <https://doi.org/10.2113/econgeo.107.3.427>
- Saade M, Araragi K, Montagner JP et al (2019) Evidence of reactivation of a hydrothermal system from seismic anisotropy changes. *Nat Commun* 10:1–8. <https://doi.org/10.1038/s41467-019-13156-8>
- Salvage RO, Avarid G, de Moor JM et al (2018) Renewed explosive phreatomagmatic activity at Poás Volcano, Costa Rica in April 2017. *Front Earth Sci* 6:1–18. <https://doi.org/10.3389/feart.2018.00160>
- Sano Y, Kagoshima T, Takahata N et al (2015) Ten-year helium anomaly prior to the 2014 Mt Ontake eruption. *Sci Rep* 5:1–7. <https://doi.org/10.1038/srep13069>
- Scolamacchia T, Cronin SJ (2016) Idiosyncrasies of Volcanic Sulfur Viscosity and the Triggering of Unheralded Volcanic Eruptions. *Front Earth Sci* 4:1–5. <https://doi.org/10.3389/feart.2016.00024>
- Seki K, Kanda W, Ogawa Y, et al (2015) Imaging the hydrothermal system beneath the Jigokudani valley, Tateyama volcano, Japan: implications for structures controlling repeated phreatic eruptions from an audio-frequency magnetotelluric survey. *Earth, Planet Sp* 67:6. <https://doi.org/10.1186/s40623-014-0169-8>
- Seropian G, Kennedy BM, Walter TR et al (2021) A review framework of how earthquakes trigger volcanic eruptions. *Nat Commun* 12:1–13. <https://doi.org/10.1038/s41467-021-21166-8>
- Simpson MP, Rosenberg MD, Rae AJ et al (2014) Insight into the 2005 hydrothermal eruption at South Orakonui, Ngatamariki Geothermal Field, New Zealand from calcite microthermometry. *New Zeal Geotherm Work 2014 Proc* 1:1–6
- Stix J, de Moor JM (2018) Understanding and forecasting phreatic eruptions driven by magmatic degassing. *Earth, Planets Sp* 70:19. <https://doi.org/10.1186/s40623-018-0855-z>
- Strehlow K, Sandri L, Gottsmann JH et al (2017) Phreatic eruptions at crater lakes: occurrence statistics and probabilistic hazard forecast. *J Appl Volcanol* 6:21. <https://doi.org/10.1186/s13617-016-0053-2>
- Sutawidjaja IS, Prambada O, Siregar DA et al (2013) The August 2010 Phreatic Eruption of Mount Sinabung, North Sumatra Letusan Freatik Gunungapi Sinabung Agustus 2010, Sumatra Utara. *Indones J Geosci* 8:55–61
- Swanson DA, Rose TR, Mueck AE et al (2014) Cycles of explosive and effusive eruptions at Kīlauea Volcano, Hawai'i. *Geology* 42:631–634. <https://doi.org/10.1130/G35701.1>
- Taddeucci J, Valentine GA, Sonder I et al (2013) The effect of pre-existing craters on the initial development of explosive volcanic eruptions: An experimental investigation. *Geophys Res Lett* 40:507–510. <https://doi.org/10.1002/grl.50176>
- Tajima Y, Nakada S, Maeno F et al (2020) Shallow Magmatic Hydrothermal Eruption in April 2018 on Ebinokogen Ioyama Volcano in Kirishima. *Geosciences* 10:1–25. <https://doi.org/10.3390/geosciences10050183>
- Taussi M, Nisi B, Pizarro M et al (2019) Sealing capacity of clay-cap units above the Cerro Pabellón hidden geothermal system (northern Chile) derived by soil CO<sub>2</sub> flux and temperature measurements. *J Volcanol Geotherm Res* 384:1–14. <https://doi.org/10.1016/j.jvolgeores.2019.07.009>
- Terada A, Kanda W, Ogawa Y, Yamada T, Yamamoto M, Ohkura T, Aoyama H, Tsutsui T, Onizawa, S (2021) The 2018 phreatic eruption at Mt. Motoshirane of Kusatsu–Shirane volcano, Japan: eruption and intrusion of hydrothermal fluid observed by a borehole tiltmeter network. *Earth, Planets Sp* 73. <https://doi.org/10.1186/s40623-021-01475-4>
- Terakawa T, Kato A, Yamanaka Y, et al (2016) Monitoring eruption activity using temporal stress changes at Mount Ontake volcano. *Nat Commun* 7:10797. <https://doi.org/10.1038/ncomms10797>
- Thiéry R, Mercury L (2009) Explosive properties of water in volcanic and hydrothermal systems. *J Geophys Res Solid Earth* 114:1–19. <https://doi.org/10.1029/2008JB005742>
- Thiéry R, Loock S, Mercury L (2010) Explosive properties of superheated aqueous solutions in volcanic and hydrothermal systems. In: Rzoska S, Drozd-Rzoska A, Mazur V (eds) *Metastable Systems under Pressure*, NATO Scien. Springer, Dordrecht, pp 293–310
- Tonini R, Sandri L, Rouwet D et al (2016) A new Bayesian Event Tree tool to track and quantify volcanic unrest and its application to Kawah Ijen volcano. *Geochem Geophys Geosyst* 17:2539–2555. <https://doi.org/10.1002/2016GC006327>
- Toramaru A, Maeda K (2013) Mass and style of eruptions in experimental geysers. *J Volcanol Geotherm Res* 257:227–239. <https://doi.org/10.1016/j.jvolgeores.2013.03.018>
- Tseng KH, Ogawa Y, Nurhasan, Tank, S.B., Ujihara, N., Honkura, Y., Terada, A., Usui, Y., Kanda, W (2020) Anatomy of active volcanic edifice at the Kusatsu–Shirane volcano, Japan, by

- magnetotellurics: hydrothermal implications for volcanic unrests. *Earth, Planets Sp* 72:161. <https://doi.org/10.1186/s40623-020-01283-2>
- Tsunematsu K, Ishimine Y, Kaneko T, et al (2016) Estimation of ballistic block landing energy during 2014 Mount Ontake eruption. *Earth, Planets Sp* 68. <https://doi.org/10.1186/s40623-016-0463-8>
- Valentine GA, Sottili G, Palladino DM, Taddeucci J (2015) Tephra ring interpretation in light of evolving maar–diatreme concepts: Stracciacappa maar (central Italy). *J Volcanol Geotherm Res* 308:19–29. <https://doi.org/10.1016/j.jvolgeores.2015.10.010>
- Valentine GA, Graettinger AH, Macorps É, et al (2015a) Experiments with vertically and laterally migrating subsurface explosions with applications to the geology of phreatomagmatic and hydrothermal explosion craters and diatremes. *Bull Volcanol* 77. <https://doi.org/10.1007/s00445-015-0901-7>
- Vaughan RG, Hungerford JDG, Keller W (2020) A Newly Emerging Thermal Area in Yellowstone. *Front Earth Sci* 8:1–19. <https://doi.org/10.3389/feart.2020.00204>
- Vialle S, Li Y, Carey JW (2018) Geological carbon storage: Subsurface seals and caprock integrity. John Wiley & Sons, Hoboken. <https://doi.org/10.1002/9781119118657>
- Walsh B, Procter J, Lokmer I, Thun J, Hurst T, Christenson B, Jolly A (2019) Geophysical examination of the 27 April 2016 Whakaari/White Island, New Zealand, eruption and its implications for vent physiognomies and eruptive dynamics. *Earth, Planets Sp* 71:25. <https://doi.org/10.1186/s40623-019-1003-0>
- Wang M, Huang Z, Zhang X et al (2021) Altered mineral mapping based on ground-airborne hyperspectral data and wavelet spectral angle mapper tri-training model: Case studies from Dehua-Youxi-Yongtai Ore District, Central Fujian, China. *Int J Appl Earth Obs Geoinf* 102:102409. <https://doi.org/10.1016/j.jag.2021.102409>
- Wu Y, Li P (2020) The potential of coupled carbon storage and geothermal extraction in a CO<sub>2</sub>-enhanced geothermal system: a review. *Geotherm Energy* 8:19. <https://doi.org/10.1186/s40517-020-00173-w>
- Yamada K (2022) A quantitative approach to the 2014 Mt. Ontake volcanic eruption news coverage: understanding the information gap and the public response to the anniversary coverage. *J Appl Volcanol* 11:1–23. <https://doi.org/10.1186/s13617-021-00113-8>
- Yamada T, Kurokawa AK, Terada A et al (2021) Locating hydrothermal fluid injection of the 2018 phreatic eruption at Kusatsu-Shirane volcano with volcanic tremor amplitude. *Earth Planets Sp* 73:1–15. <https://doi.org/10.1186/s40623-020-01349-1>
- Yamamoto M, Goto T, nori, Kiji M, (2017) Possible mechanism of molten sulfur eruption: Implications from near-surface structures around of a crater on a flank of Mt. Shiretokoiozan, Hokkaido. *Japan J Volcanol Geotherm Res* 346:212–222. <https://doi.org/10.1016/j.jvolgeores.2017.11.009>
- Yates AS, Savage MK, Jolly AD et al (2019) Volcanic, Coseismic, and Seasonal Changes Detected at White Island (Whakaari) Volcano, New Zealand, Using Seismic Ambient Noise. *Geophys Res Lett* 46:99–108. <https://doi.org/10.1029/2018GL080580>
- Yoshimura R, Ogawa Y, Yukutake Y et al (2018) Resistivity characterisation of Hakone volcano, Central Japan, by three-dimensional magnetotelluric inversion. *Earth, Planets Sp* 70:1–10. <https://doi.org/10.1186/s40623-018-0848-y>
- Zhang M, Wen L (2015) Earthquake characteristics before eruptions of Japan's Ontake volcano in 2007 and 2014. *Geophys Res Lett* 42:6982–6988. <https://doi.org/10.1002/2015GL065165>